Published in final edited form as:
Cell Microbiol. 2010 October ; 12(10): 1517–1533. doi:10.1111/j.1462-5822.2010.01487.x.

Sphingomyelin is Important for the Cellular Entry and Intracellular Localization of *Helicobacter pylori* VacA

Vijay R. Gupta, **Brenda A. Wilson**, and **Steven R. Blanke***
Department of Microbiology, Institute for Genomic Biology, University of Illinois, B103 CLSL, 601 South Goodwin Avenue. Urbana, IL 61801

Summary

Plasma membrane sphingomyelin (SM) binds the *Helicobacter pylori* vacuolating toxin (VacA) to the surface of epithelial cells. To evaluate the importance of SM for VacA cellular entry, we characterized toxin uptake and trafficking within cells enriched with synthetic variants of SM, whose intracellular trafficking properties are strictly dependent on the acyl chain lengths of their sphingolipid backbones. While toxin binding to the surface of cells was independent of acyl chain length, cells enriched with 12- or 18-carbon acyl chain variants of SM (e.g. C12-SM or C18-SM) were more sensitive to VacA, as indicated by toxin-induced cellular vacuolation, than those enriched with shorter 2- or 6-carbon variants (e.g. C2-SM or C6-SM). In C18-SM enriched cells, VacA was taken into cells by a previously described Cdc42-dependent pinocytic mechanism, localized initially to GPI-enriched vesicles, and ultimately trafficked to Rab7/Lamp1 compartments. In contrast, within C2-SM enriched cells, VacA was taken up at a slower rate by a Cdc42-independent mechanism and trafficked to Rab11 compartments. VacA associated predominantly with detergent-resistant membranes (DRMs) in cells enriched with C18-SM, but predominantly with non-DRMs in C2-SM enriched cells. These results suggest that SM is required for targeting VacA to membrane rafts important for subsequent Cdc42-dependent pinocytic cellular entry.

Keywords

VacA; sphingomyelin; receptor; trafficking; *Helicobacter*

Introduction

Chronic infection with the gastric pathogen *Helicobacter pylori* is a significant risk factor for the development of peptic ulcer disease, distal gastric adenocarcinoma, and gastric lymphoma in humans (Cover and Blaser, 2009; Suerbaum and Josenhans, 2007). The vacuolating cytotoxin (VacA) is an intracellular-acting toxin that is important for *Helicobacter pylori* colonization and disease pathogenesis (Fujikawa *et al.*, 2003; Salama *et al.*, 2001; Telford *et al.*, 1994). Intoxication of epithelial cells with VacA results in multiple consequences, including vacuolation and apoptosis (Cover and Blanke, 2005).

VacA is internalized into epithelial cell lines by a Cdc42-dependent pinocytic mechanism, and is trafficked to late endosomal/lysosomal compartments (Gauthier *et al.*, 2007; Gauthier *et al.*, 2006; Gauthier *et al.*, 2005; McClain *et al.*, 2000; Molinari *et al.*, 1997; Papini *et al.*, 1997). As the first step during cellular intoxication, VacA binds to the plasma membrane of

*Corresponding author: Steven R. Blanke, Ph.D. Department of Microbiology Institute for Genomic Biology University of Illinois B103 CLSL 601 South Goodwin Avenue Urbana, IL 61801. Telephone: (217) 244-2412 Fax: (217) 244-6697 sblanke@life.uiuc.edu.

sensitive cells (Garner and Cover, 1996), analogous to other intracellular-acting bacterial toxins (Blanke, 2006). Recently, sphingomyelin (SM) was identified as a plasma membrane receptor that confers cellular sensitivity to VacA by binding the toxin to the cell surface (Gupta *et al.*, 2008). However, this previous study did not address whether SM is required also for Cdc42-dependent pinocytic uptake from the plasma membrane and trafficking of VacA to late endosomal/lysosomal compartments.

The purpose of this study was to evaluate whether, subsequent to binding VacA to the cell surface (Gupta *et al.*, 2008), SM might also be important for toxin internalization and/or intracellular trafficking. To investigate this possibility, we studied the internalization of VacA into cells enriched with synthetic variants of SM, whose intracellular trafficking properties are strictly dependent on the length of the sphingolipid backbone acyl chain (Koivusalo *et al.*, 2007). These studies revealed that although toxin binding was independent of SM acyl chain length, cells enriched with 12- or 18-carbon acyl chain variants of SM (C12-SM or C18-SM, respectively) were more sensitive to VacA than cells enriched with shorter 2- or 6-carbon variants (C2-SM or C6-SM, respectively). In C18-SM enriched cells, VacA was internalized by a previously described Cdc42-dependent pinocytic mechanism, localized initially to GPI-enriched vesicles, and then trafficked to Rab7/Lamp1 rich compartments (Gauthier *et al.*, 2007; Gauthier *et al.*, 2006; Gauthier *et al.*, 2005; Gauthier *et al.*, 2004). In contrast, using C2-SM enriched cells, VacA was taken up at a slower rate by a Cdc42-independent mechanism and trafficked to Rab11 rich compartments. Finally, VacA was demonstrated to associate predominantly with detergent-resistant membranes (DRMs) in cells enriched with C18-SM, but predominantly with non-DRMs in cells enriched with C2-SM. These results suggest that SM is required for the targeting of VacA to membrane rafts and subsequent Cdc42-dependent pinocytic cellular entry and subsequent trafficking to late endosomal/lysosomal compartments.

Results

Plasma membrane SM is taken up into VacA-containing intracellular compartments

Our earlier work demonstrated the importance of SM for binding VacA to the surface of mammalian cells (Gupta *et al.*, 2008), but did not address the requirement for SM during subsequent steps of intoxication. If plasma membrane SM is important for VacA entry into cells, then it is reasonable to predict that both toxin and sphingolipid are taken up into the same intracellular compartment. To evaluate this possibility, monolayers of AZ-521 human-derived gastric cells, which have been extensively used to investigate VacA interactions with epithelial cells (Nakayama *et al.*, 2006; Nakayama *et al.*, 2004; Yahiro *et al.*, 1999; Yahiro *et al.*, 1997), were pre-chilled on ice and then incubated with pre-chilled Venus-lysenin, a fluorescent version of a SM-binding protein from earthworm (Kiyokawa *et al.*, 2005), and either Alexa Fluor 647-labeled VacA, or, Alexa fluor 568 labeled-transferrin (as an unrelated control). During the incubation period on ice, fluorescence microscopy confirmed the absence of intracellular VacA, transferrin, or lysenin, (data not shown). After 1 h, the cells were washed to remove unbound proteins, and further incubated at 37 °C to allow internalization. After 30 min, fluorescence microscopy revealed visible puncta of co-localized VacA and Venus-lysenin (Fig. 1A), indicating that plasma membrane SM and VacA were present in the same intracellular vesicles, and supporting the idea that during toxin internalization, SM is taken up along with VacA from the cell surface. Intracellular co-localization of VacA with Venus-lysenin was apparent 10 min after warming the cells to 37 °C (data not shown), indicating that uptake of surface-bound toxin and SM occurs rapidly after switching to conditions permissive for cellular entry. Venus-lysenin co-localized with transferrin-containing vesicles to a significantly lower degree than VacA-containing vesicles (Fig. 1A, B), suggesting that plasma membrane SM is not internalized to the same extent in all protein uptake pathways.

VacA-mediated cellular vacuolation, but not binding, is dependent on SM acyl chain length

An earlier study reported that VacA binding to the surface of cells is strongly correlated to SM levels, as the depletion of plasma membrane SM with the membrane impermeable sphingomyelinase C (SMase C) resulted in a dose-dependent reduction in toxin binding (Gupta *et al.*, 2008). However, the use of cells depleted in plasma membrane SM for studying VacA internalization is problematic, because the low levels of surface-bound toxin available for uptake results in nearly undetectable levels of intracellular VacA (Gupta *et al.*, 2008). As an alternative strategy for ascertaining a potential functional role for SM during cellular entry, we investigated the internalization of VacA into cells enriched with synthetic variants of SM whose intracellular trafficking properties are dependent on the length of the sphingolipid backbone acyl chain (Koivusalo *et al.*, 2007). Specifically, 12- and 18- carbon acyl chain variants (C12-SM and C18-SM, respectively) were reported to be trafficked preferentially from the plasma membrane to late endosomal-like vesicles along the degradation pathway, whereas shorter 2- and 6- carbon acyl chain variants (C2-SM and C6-SM, respectively) were demonstrated to be trafficked preferentially to recycling compartments (Koivusalo *et al.*, 2007). Although a distribution of SM acyl chain length variants normally exists within biological membranes, the longer chain variants, and in particular C16-SM and C18-SM, are typically more abundant than short chain variants (Valsecchi *et al.*, 2007; Barenholz, 1984). Because VacA induces vacuole biogenesis from within late endosomal/lysosomal compartments (Genisset *et al.*, 2007; Gauthier *et al.*, 2005; Papini *et al.*, 1997), we predicted that if SM is important for the uptake and trafficking of toxin to these intracellular compartments, then cells enriched in C12-SM or C18-SM, which are normally trafficked preferentially from the plasma membrane to late endosomes, would be more susceptible to VacA than cells enriched in C2-SM or C6-SM, which are typically trafficked from the plasma membrane to recycling compartments. Alternatively, we predicted that if the importance of SM does not extend beyond binding VacA to the plasma membrane, then cellular intoxication should be independent of SM acyl chain length.

Prior to evaluating the requirement of SM for VacA uptake and intracellular trafficking, it was important to first compare VacA binding to cells enriched with each SM acyl chain variant. The SM headgroup for each variant used in this study was phosphorylcholine, which had earlier been demonstrated to be important for VacA interactions (Gupta *et al.*, 2008), leading us to predict that VacA binding to the plasma membrane of SM-enriched cells should be independent of backbone acyl chain length. To test this prediction, we measured VacA binding to monolayers of AZ-521 cells enriched with C2-SM, C6-SM, C12-SM, C18-SM, or a non-synthetic preparation of membrane extracted SM with normal variance in acyl chain lengths (hereafter referred to as “membrane extracted-SM”). In preliminary studies, we confirmed our previous work using other cell lines (Gupta *et al.*, 2008), by demonstrating that the overall binding of VacA to the surface of AZ-521 cells is strictly dependent on cellular SM levels (Fig. S1, Fig. S2, Table S1). However, these current studies revealed that nearly identical levels of VacA were bound to the surface of cells enriched in C2-SM, C6-SM, C12-SM, C18-SM, or membrane extracted-SM (Fig. 2A). Similar data were obtained using HeLa cells (data not shown), indicating that these findings were not idiosyncratic to AZ-521 cells. These results confirmed that VacA binding to cells is independent of SM acyl chain length, thus setting the stage for evaluating the sensitivity of these same cells to VacA under conditions where equal amounts of toxin are bound to the cell surface.

To evaluate whether or not VacA cellular activity is dependent on SM acyl chain length, we measured toxin-mediated vacuolation of AZ-521 cells enriched with C2-SM, C6-SM, C12-SM, or C18-SM. In preliminary studies, we demonstrated that the sensitivity of AZ-521 cells to VacA is strictly dependent on SM levels (Fig. S3-Fig. S6, Table S1), which confirmed our previous work using other cell lines (Gupta *et al.*, 2008). These current experiments revealed that VacA induced visibly (Fig. 2B) and quantitatively (Fig. 2C) more vacuolation of cells enriched with C12-SM or C18-SM than of cells enriched with C2-SM or C6-SM. Similar results were obtained using HeLa cells (data not shown). The decreased vacuolation detected within C2-SM and C6-SM enriched cells was not due to depleted sphingolipid within these cells, as each of the SM acyl chain length variants was incorporated into SMase C pretreated cells to approximately the same extent (Fig. S7). These results indicated that, in contrast to plasma membrane binding (Fig. 2A), VacA-dependent vacuolation was strictly dependent on SM acyl chain length, suggesting that SM is important for VacA intoxication pathway at steps beyond toxin binding. Because cells enriched with C2-SM or C18-SM yielded the greatest contrast in cell sensitivity to VacA, we used these two variants in subsequent studies of toxin uptake and trafficking.

The rate, but not overall amount, of VacA uptake into cells is sensitive to variation in SM acyl chain length

To evaluate the possibility that SM might be important for the overall levels of VacA taken into cells, we measured toxin internalization into AZ-521 cells enriched in either C2-SM or C18-SM. These experiments revealed that within C2-SM or C18-enriched cells, similar amounts of VacA had been internalized at 30, 60, and 120 min (Fig. 3). However, at 5 and 15 min, significantly less VacA was detected within cells enriched with C2-SM than in cells with C18-SM. These results indicated that the initial rate at which VacA is taken up into cells from the plasma membrane is dependent on SM acyl chain length, and supports the idea that plasma membrane SM impacts the uptake pathway by which VacA enters cells.

VacA uptake is sensitive to variation in SM acyl chain length

The difference in the rates of VacA internalization from the surface of cells enriched in C2-SM or C-18 (Fig. 3) suggested that SM might influence the overall pathway by which VacA is taken into cells. To evaluate this possibility, we compared VacA localization to intracellular compartments containing the fluid phase marker Texas-Red-dextran, which was reported previously to accompany the pinocytic uptake of VacA (Gauthier *et al.*, 2005). These studies revealed that after 10 min, significantly more VacA co-localized with Texas-Red-dextran in cells enriched with C18-SM, similar to mock-pretreated cells, than in cells enriched with C2-SM (Fig. 4A). The VacA/dextran colocalization index in C2-SM enriched cells did not increase at later time points (up to 2 h; data not shown), indicating that the relatively low amount of VacA/dextran colocalization in C2-SM enriched cells at 10 min relative to C18-SM enriched cells is not likely due to differences in the initial rates of toxin uptake (Fig. 3).

Shortly after uptake from the plasma membrane, VacA localizes to GPI-anchored protein enriched endosomal compartments, called GEECs (Gauthier *et al.*, 2005). To further evaluate the relationship between plasma membrane SM and the cellular uptake pathway of VacA, we compared VacA localization to GEECs in cells that had been enriched with either C2-SM or C18-SM. In these studies, we used DIC/fluorescence microscopy to determine VacA co-localization with fluorescent aerolysin (ASSP), which is a commonly used pan GPI-anchored protein probe (Fivaz *et al.*, 2002). These studies revealed significantly more VacA co-localized with ASSP in cells enriched with C18-SM than in cells enriched with C2-SM (Fig. 4B). In C2-SM enriched cells, the VacA/ASSP colocalization index did not increase at later time points (up to 2 h; data not shown). Taken together, these results indicated that longer acyl chain SM promotes VacA uptake into vesicles enriched in fluid phase and GPI-anchored proteins to a greater extent than shorter chain length SM, and provide further support for the idea that plasma membrane SM influences the uptake pathway by which VacA enters cells.

The Cdc42-dependence of VacA uptake is sensitive to variation in SM acyl chain length

The small GTP-binding protein Cdc42 was previously reported to be important for the uptake of VacA into cells and toxin-dependent vacuolation (Gauthier *et al.*, 2005). To evaluate the importance of plasma membrane SM for Cdc42-dependent entry of VacA, we compared VacA internalization into either C2-SM or C18-SM enriched AZ-521 cells that had been transiently transfected with an expression plasmid containing the gene encoding a dominant-negative form of Cdc42 (Cdc42 (T17N)-GFP), which had earlier been demonstrated to inhibit VacA uptake into cells (Gauthier *et al.*, 2005). These studies revealed that for both C18-SM enriched cells and mock-pretreated cells, there were considerably fewer intracellular VacA-containing vesicles in transfected cells than in non-transfected cells (Fig. 5A), as indicated by the presence or absence of GFP fluorescence, respectively. In contrast, an approximately equal number of VacA-containing vesicles were detected in transfected and non-transfected cells enriched in C2-SM (Fig. 5A), suggesting that for cells enriched in short chain acyl variants, VacA uptake was not Cdc42 dependent. Internalization of transferrin (as an unrelated control) was not sensitive to dominant-negative Cdc42-GFP in AZ-521 cells enriched in either C2-SM or C18-SM (Fig. 5B). These results indicated that longer acyl chain SM promotes a Cdc42-dependent uptake mechanism, as previously described for VacA (Gauthier *et al.*, 2005), and suggests that plasma membrane SM influences the mechanism by which VacA taken up from the cell surface.

Localization of VacA to intracellular compartments is sensitive to variation in SM acyl chain length

The differences observed in VacA uptake between cells enriched in C2-SM or C18-SM (Fig. 4, 5) suggested that intracellular trafficking of VacA might also be dependent on SM. Previously, trafficking of VacA to compartments rich in late endosomal (Rab7) and lysosomal (Lamp1) markers was demonstrated to be required for toxin dependent cellular vacuolation (Gauthier *et al.*, 2007;Gauthier *et al.*, 2005;Molinari *et al.*, 1997;Ricci *et al.*, 1997;Papini *et al.*, 1994). To evaluate the importance of plasma membrane SM for intracellular trafficking of VacA to late endosomal compartments, we investigated VacA localization to Rab7-rich vesicles in AZ-521 cells enriched in either C2-SM or C18-SM. DIC/fluorescence microscopy revealed that at 60 min, significantly more VacA had localized to Rab7-associated vesicles in C18-SM enriched cells or mock-pretreated cells than in C2-SM enriched cells (Fig. 6A). Likewise, significantly more VacA has localized to Lamp1-associated vesicles (Fig. S8) in C18-SM enriched cells or mock-pretreated cells than in C2-SM enriched cells (Gauthier *et al.*, 2007;Li *et al.*, 2004;Molinari *et al.*, 1997;Papini *et al.*, 1994). These results are consistent with the idea that plasma membrane SM targets VacA to the uptake and trafficking pathway required for toxin action (Ricci *et al.*, 1997;Papini *et al.*, 1994).

The relatively low levels of VacA cellular activity (Fig. 2B, C) and toxin localization to late endosomal/lysosomal compartments (Fig. 6A, S8) in C2-SM enriched cells compared to cells enriched with C18-SM suggested that, subsequent to binding and uptake, VacA trafficking may be fundamentally different in cells enriched in long- or short- acyl chain length variants of SM. Notably, short acyl chain variants of SM (e.g. C2-SM, C6-SM) were previously demonstrated to be trafficked preferentially from early endosomal compartments to recycling compartments (Koivusalo *et al.*, 2007). To evaluate the possibility that subsequent to uptake into C2-SM enriched cells, VacA is routed preferentially to recycling compartments, we examined the relative localization of VacA with Rab11-associated recycling vesicles (Lakadamyali *et al.*, 2006) in AZ-521 cells enriched with either C2-SM or C18-SM. These experiments revealed significantly more VacA localization to Rab11-associated vesicles in C2-SM enriched cells than in either C18-SM enriched cells or mock-pretreated cells (Fig. 6B). VacA localization within C18-SM or C2-SM enriched cells at 60 min (Fig. 6B) was very similar to those observed at 120 min (data not shown).

Control experiments revealed that localization of epidermal growth factor (EGF) to Rab7/ Lamp1 associated compartments was essentially identical in cells enriched in C2-SM or C18-SM (data not shown), validating that the normal trafficking of EGF from the cell surface to late endosomes (Futter *et al.*, 1996) is independent of SM acyl chain length. These results also suggest that the apparent re-routing of VacA to Rab11-associated recycling vesicles cannot readily be explained by inactivation of all protein trafficking along the late endosomal/lysosomal degradation pathway within C2-SM enriched cells.

Partitioning of VacA into membrane raft and non-raft domains of the plasma membrane

The differences observed between the cell entry (Fig. 4,5) and routing (Fig. 6) pathways of VacA within cells enriched in C2-SM or C-18 suggested that, prior to uptake, VacA association with SM on the surface of these cells might be fundamentally different. We hypothesized that the acyl chain variants might affect the association of VacA with membrane rafts on the surface of sensitive cells, which previous studies have indicated to be important for toxin function (Gupta *et al.*, 2008;Nakayama *et al.*, 2006;Geisse *et al.*, 2004b;Geisse *et al.*, 2004a;Patel *et al.*, 2002;Schraw *et al.*, 2002). To evaluate this possibility, we investigated VacA association with DRMs, which are the biochemical correlates of membrane rafts, in cells that had been enriched with C2-SM, C12-SM, or C18-SM, taking advantage of our finding that overall toxin binding to cells is independent of SM acyl chain length (Fig. 2A). These experiments revealed that for both C18-SM enriched cells and mock-pretreated cells, approximately 80% of the total membrane-bound VacA was detected in low-density DRMs (Fig. 7A, B), as previously reported in studies using a number of different cell lines (Gupta *et al.*, 2008;Patel *et al.*, 2002;Schraw *et al.*, 2002). In contrast, nearly equivalent amounts of VacA were detected in DRMs and non-DRM fractions prepared from C12-enriched cells, while in cells enriched with C2-SM, VacA was detected predominantly in the less buoyant fractions near the bottom of the gradient, suggesting that the toxin was associated primarily with non-ordered domains within the lipid bilayer. When cells with bound VacA were incubated at 37 °C for 30 min to allow for uptake of the toxin from the plasma membrane and intracellular transport, we again detected VacA predominantly in the low-density DRMs from C18-SM enriched cells and mock-pretreated cells (data not shown). These results were consistent with an earlier report indicating that VacA-association with rafts is not substantially altered during the early stages of endocytosis (Nakayama *et al.*, 2006). Likewise, VacA remained associated predominantly with less buoyant membrane fractions from cells enriched with C2-SM (data not shown), suggesting VacA had not partitioned into membrane rafts during the early stages of endocytosis in these cells. The association of the membrane raft marker flotillin with DRMs was similar in cells enriched with C18-SM, C12-SM, or C2-SM (Fig. 7A), indicating that variations in SM acyl chain length does not alter the membrane distribution of all raft-associated proteins. Consistent with results obtained from flow cytometric analysis (Fig. 2A), the overall amount of cell-associated VacA was largely independent of SM acyl chain length (Fig. 7C). Interestingly, based on our findings that the total amount of VacA internalized is independent of acyl chain length (Fig. 3), our data indicate that VacA is taken up into cells regardless of whether the toxin is associated with raft or non-raft domains of the plasma membrane. However, our results also support a model where SM-dependent targeting of surface-bound VacA into membrane raft domains is required for the uptake pathway and intracellular routing of VacA required for toxin activity.

Discussion

The susceptibility of eukaryotic cells to intracellular-acting bacterial toxins is largely dictated by the availability of specific toxin receptors (Blanke, 2006). Recently, we identified SM as a plasma membrane receptor that confers sensitivity to VacA by binding the toxin to the cell surface (Gupta *et al.*, 2008). However, this previous study did not address whether SM is required also for subsequent Cdc42-dependent pinocytic uptake and trafficking of VacA to late endosomal/lysosomal compartments, which is important for toxin mediated vacuolating activity.

Our results here indicated that SM is required for targeting VacA to the uptake pathway previously demonstrated to be important for cellular intoxication. Using cells enriched with synthetic variants of SM that each binds VacA to the same extent, we observed that the properties of toxin uptake and intracellular localization was strictly dependent on SM acyl chain length. Cells enriched with C18-SM, which is naturally abundant in biological membranes (Valsecchi *et al.*, 2007; Barenholz, 1984), took up and localized toxin by a previously described Cdc42-dependent pinocytic pathway into GEECs (Fig. 4, 5) (Gauthier *et al.*, 2005; Sabharanjak *et al.*, 2002), and then trafficked to late endosomal/lysosomal vesicles (Fig. 6), which had previously been demonstrated to be important for toxin-mediated cellular vacuolation (Gauthier *et al.*, 2007; Gauthier *et al.*, 2006; Gauthier *et al.*, 2005; McClain *et al.*, 2000; Molinari *et al.*, 1997; Papini *et al.*, 1997). In contrast, VacA internalization and localization was fundamentally different within cells enriched with C2-SM, which is typically present at very low abundance within biological membranes (Valsecchi *et al.*, 2007; Barenholz, 1984), as toxin was taken into cells at a slightly slower rate (Fig. 3) by a Cdc42-independent mechanism (Fig. 5) and trafficked to Rab11-associated recycling compartments (Fig. 6). We did not further characterize the uptake of VacA into C2-SM enriched cells, as there is no existing evidence that this pathway is normally important during VacA intoxication.

How might SM-dependent association of VacA with the plasma membrane promote toxin internalization by a Cdc42-dependent pinocytic pathway into GEECs? SM was earlier reported to be essential for VacA association with membrane rafts (Gupta *et al.*, 2008), and rafts had earlier been reported to be important for toxin internalization (Gupta *et al.*, 2008; Nakayama *et al.*, 2006; Gauthier *et al.*, 2005; Geisse *et al.*, 2004a; Patel *et al.*, 2002; Schraw *et al.*, 2002). Our studies here revealed for the first time that SM-mediated partitioning of VacA between raft and non-raft domains on the plasma membrane surface is strictly dependent on acyl chain length (Fig. 7). Several studies have demonstrated that longer SM acyl chain variants (C-18 and above) partition preferentially into ordered gel domains, while shorter chain variants (C-10 and below) partition into disordered fluid domains (Koivusalo *et al.*, 2007; Niemela *et al.*, 2006; Koivusalo *et al.*, 2004; van Meer and Lisman, 2002). Interestingly, our finding that overall levels of internalized VacA were approximately the same in C2-SM and C18-SM enriched cells (Fig. 3) indicates that toxin association with plasma membrane rafts is not strictly required for the internalization of VacA into cells. Nonetheless, as discussed below, our data are consistent with a model that SM-dependent association of VacA with rafts is required for the targeting of the toxin for the Cdc42-dependent uptake pathway associated with VacA intracellular activity.

A potential mechanistic role for SM in Cdc42-dependent pinocytosis was previously suggested by studies demonstrating that depletion of SM from the surface of Chinese hamster ovary (CHO) cells using SMase C inhibited the targeting of Cdc42 to membrane rafts within the plasma membrane required for the uptake of the fluid phase marker dextran (Cheng *et al.*, 2006). Supplementation of SMase C pretreated CHO cells with exogenous SM, but not ceramide, monosialoganglioside GM3, or lactosylceramide, restored cellular uptake of dextran and plasma membrane targeting of Cdc42 (Cheng *et al.*, 2006). Although we did not investigate SM-dependent Cdc42 membrane recruitment within VacA-intoxicated cells, we speculate that SM may target VacA to membrane rafts containing the effector molecules required for uptake of the toxin by the Cdc42-dependent pathway.

Several groups have reported that cell surface GPI-anchored proteins are required for efficient cellular entry and vacuolating activity of VacA (Gauthier *et al.*, 2005; Gauthier *et al.*, 2004; Kuo and Wang, 2003; Ricci *et al.*, 2000). Our studies revealed that the uptake of VacA along with GPI-anchored proteins is dependent on SM acyl chain length (Fig. 4), suggesting that both SM and GPI-anchored proteins might be required for targeting VacA to GEECs. GPI-anchored proteins are not likely receptors for VacA, as they are not required for required either cell binding or membrane raft association (Gauthier *et al.*, 2005; Gauthier *et al.*, 2004; Kuo and Wang, 2003; Schraw *et al.*, 2002). In addition, VacA does not induce an increase in fluid phase uptake, nor is toxin uptake inhibited by a blocker of macropinocytosis (Gauthier *et al.*, 2005), suggesting that the toxin uptake pathway to GEECs is not induced by VacA cell binding. One model is that VacA exploits an existing mechanism for the recycling of plasma membrane GPI-anchored proteins, for which the level of membrane targeting to GEECs is dependent on the level of GPI-anchored proteins on the plasma membrane (Gauthier *et al.*, 2005). Future studies will be required to clarify the relationship between SM-dependent internalization of VacA to GEECs and the potentiation of VacA cellular activity by GPI-anchored proteins.

Trafficking of VacA to Rab7/Lamp1 enriched intracellular compartments is important for VacA cellular activity (Gauthier *et al.*, 2007; Gauthier *et al.*, 2005; Molinari *et al.*, 1997; Ricci *et al.*, 1997; Papini *et al.*, 1994). Our results here suggest that VacA-SM interactions on the plasma membrane are important for the targeting of toxin to these intracellular compartments along the degradation pathway. Toxin-mediated vacuole biogenesis is dependent on VacA channel formation in the late endosomal membrane, which has been proposed to activate the vacuolar ATPase (V-ATPase) proton pump resulting in the accumulation of osmotic species such as NH_4Cl and late endosomal swelling (Cover and Blanke, 2005; Gauthier *et al.*, 2004; Papini *et al.*, 2001). Active V-ATPase requires both the transmembrane Vo domain and cytosolic V_1 domain, and recent studies indicated that ratio of membrane associated V_1/Vo varies along with the endocytic pathway, with a higher relative amount of V1 associated with late endosomes than other endosomal compartments (Lafourcade *et al.*, 2008), perhaps explaining the importance of VacA trafficking to late endosomes for toxin-mediated cellular vacuolation to occur. Previous studies suggested a direct link between sphingolipids and membrane assembly and maturation of functional V-ATPase in yeast (Chung *et al.*, 2003), but it is unclear whether or not SM has any direct role in activating V-ATPase in mammalian cells during VacA intoxication.

The stability of SM acyl chains, and in particular, those of exogenously added SMs, was not experimentally addressed in this study. However, eukaryotic cells have not been reported to modify the acyl chains of intact SM molecules (Milhas *et al.*, 2009). Instead, the acyl chains are added during biosynthesis of the SM precursor, ceramide, which occurs at the cytoplasmic leaflet of the endoplasmic reticulum (Merrill, 2002). Thus, we suspect that the acyl chain lengths of the exogenous SMs used in these studies remained unchanged during the course of toxin binding and uptake.

In summary, our results strongly suggest that the function of SM as a VacA receptor extends beyond binding the toxin to the cell surface. Our current model is that SM targets VacA to membrane rafts required for Cdc42-dependent pinocytic cellular entry and subsequent trafficking to late endosomal/lysosomal compartments. Current studies are focused on identifying SM-dependent raft components required for toxin uptake, as well as the cellular factors required for sorting VacA within early cellular compartments to the degradation pathway.

Experimental Procedures

Purification of VacA

Helicobacter pylori 60190 (49503; ATCC; Manassas, VA), were cultured, and VacA was purified as described previously (Cover *et al.*, 1997).

Cell culture

AZ-521 cells (3940; Japan Health Science Foundation) or HeLa cells (CCL-2; ATCC) were maintained within a humidified atmosphere under 5% CO_2 at 37 °C in "complete cell medium," which is defined as minimum essential medium (MEM; Sigma; St. Louis, MO) supplemented with 2 mM glutamine, 50 U penicillin/mL, 50 μg streptomycin sulfate/mL (Sigma), and 10% fetal bovine calf serum (FBS; JRH Biosciences, Lenexa, KS). To deplete plasma membrane SM, cells were pre-incubated with the indicated concentrations of bacterial sphingomyelinase C (SMase C; Sigma) followed by washing with ice-cold complete cell medium to remove SMase C. Cells were then incubated further with membrane extracted sphingomyelin (SM), phosphatidylcholine (PC), phosphatidylethanolamine (PE), phosphatidylinositol (PI), acetyl sphingomyelin (C2-SM), hexanoyl sphingomyelin (C6-SM), lauroyl sphingomyelin (C12-SM), stearoyl sphingomyelin (C18-SM) (all from Avanti Polar Lipids; Alabaster, AL), or, cholesterol (Sigma), at 4 °C for 30 min prior to intoxication. For controls, cells were mock pretreated with PBS pH 7.2. Cells were never exposed to greater than 1% solvent (DMSO/methanol 1:1). As quality control, it was established that incubation with the lipid preparations used in these studies did not cause an increase in AZ-521 cell death (data not shown), as indicated by a commercial live/dead assay (Invitrogen/Molecular Probes; Eugene, OR).

Preparation of Venus-lysenin and non-toxic ASSP

The plasmid harboring the gene encoding nontoxic ASSP was obtained as a gift from Dr. F. Van der Goot, and the recombinant nontoxic ASSP was expressed in *E. coli* BL21(DE3) (Novagen; Madison, WI) and purified as described (Fivaz *et al.*, 2002). The plasmid harboring the gene encoding Venus-lysenin was a gift from Dr. E. Kiyokawa (Osaka U., Jp), and the reombinant protein was expressed in *E. coli* BL21 and purified as described (Kiyokawa *et al.*, 2005).

Cell vacuolation

VacA was activated as described (de Bernard *et al.*, 1995), and added to cells in the presence of 5 mM NH_4Cl (Cover *et al.*, 1992). Monolayers were visually examined using a Fisher Scientific MicroMaster inverted light microscope (Fisher Scientific; Pittsburgh, PA), outfitted with a Nikon Coolpix 43000 camera. For quantitative analysis, neutral red uptake was measured, as previously described (Cover *et al.*, 1991). Relative vacuolation was calculated by dividing neutral red uptake of SMase C and/or lipid pretreated cells by neutral red uptake of cells incubated with VacA alone. For all experiments, neutral red uptake of mock-treated cells (e.g. minus VacA) was subtracted from the neutral red uptake of cells incubated with VacA.

SM quantification

SM levels were measured using the Amplex® Red Sphingomyelinase Assay Kit (Invitrogen/Molecular Probes; Eugene, OR), according to manufacturer's instructions (He *et al.*, 2002). Known concentrations of membrane extracted SM, C2-SM, C6-SM, C12-SM and C18-SM were used as standards. As a standard quality control measure, cellular SM levels were quantified for every experiment involving depletion or supplementation of cellular SM.

Labeling VacA and ASSP

Purified VacA and ASSP were conjugated with Alexa Fluor 488, Alexa Fluor 647, or Alexa Fluor 568, using the Alexa Fluor labeling kit (Invitrogen) according to the manufacturer's instructions. Labeling was experimentally determined not to alter VacA-mediated cellular vacuolation activity. Alexa Fluor 568 labeled-transferrin and Alexa Fluor 488 labeled-EGF were from Invitrogen.

DIC-epifluorescence Microscopy

Chamber slides were analyzed using a Delta Vision RT microscope (Applied Precision; Issaquah, WA), EX 490/20 and EM 528/38, EX 555/28 and EM 617/73, EX 640/20 and EM 685/40, using an Olympus Plan Apo 60× oil objective with NA 1.42 and working distance of 0.17 mm. DIC images were collected using a Photometrics CoolSnap HQ camera; (Photometrics, Tucson; AZ). Images were processed using SoftWoRX Explorer Suite (version 3.5.1, Applied Precision Inc; Issaquah, WA). Deconvolution was carried out using SoftWoRX constrained iterative deconvolution tool (ratio mode).

Flow cytometry

Analytical flow cytometry was carried out using a Coulter EPICS XL-MCL™ flow cytometer (Beckman Coulter, Inc.; Fullerton, CA) equipped with a 70-mm nozzle, 488 nm line of an air-cooled argon-ion laser, and 400 mV output. The band pass filter used for detection of cell fluorescence was 525/10 nm. Cell analysis was standardized for scatter and fluorescence by using a suspension of fluorescent beads. Events were recorded on a log fluorescence scale and the geometric mean fluorescence values were determined using FCS Express 3.00.0311 V Lite Standalone. The data was obtained from at least 10,000 events per sample, gated so that only cells, which were evident by their forward and side scatter properties, were considered, while non-cellular debris (relatively lower forward and side scatter properties) were excluded from analysis.

VacA binding and internalization

AZ-521 cells were pre-incubated in the absence or presence of SMase C (50 mU/mL) at 37 °C. After 1 h, the monolayers were washed with ice-cold complete medium to remove SMase C. The SMase C-treated cells were then further incubated on ice in the absence or presence of pre-chilled C2-SM, C6-SM, C12-SM, C18-SM, or membrane extracted SM (25 μM, unless otherwise indicated). After 30 min, the cells were further incubated, as indicated, with activated Alexa Fluor 488-labeled VacA (50 nM), activated Alexa Fluor 647-labeled VacA (50 nM), Alexa Fluor 568-labeled transferrin (60 nM), or Venus-lysenin (1 μM). In studies to investigate the rate of VacA internalization, Alexa Fluor 488-labeled VacA (50 nM) was used.

For studies using DIC/epifluorescence microscopy, experiments were performed with monolayers of cells in 8-well chamber slides (Nunc; Rochester, NY). For binding, cells were washed once with ice-cold PBS pH 7.2, fixed with paraformaldehyde (4%) on ice. For internalization studies, cells were washed once with ice-cold PBS pH 7.2, and then incubated at 37 °C in complete cell medium (pre-warmed to 37 °C containing unlabeled VacA, 50 nM, to maintain exposure to VacA during internalization). After indicated time points, cells were fixed with paraformaldehyde (4%) on ice.

For studies using flow cytometry, experiments were carried out with suspended cells (10^6 cells/mL). For binding studies, cells were washed once with ice-cold PBS pH 7.2, and analyzed by flow cytometry. For internalization studies, the cells were incubated on ice for 5 min in the absence or presence of trypan blue (0.5% in PBS pH7.2), which is a membrane-impermeable, Alexa Fluor 488 fluorescence-quenching agent (Hed *et al.*, 1987; Sahlin *et al.*, 1983), and then analyzed immediately by flow cytometry. Relative binding or internalization was calculated by dividing the geometric mean fluorescence of SMase C- and lipid-pretreated cells by the geometric mean fluorescence of cells incubated with VacA alone. For kinetic studies, data were plotted as a fraction of internalized VacA (+ trypan blue) versus surface VacA (− trypan blue) at each time point between mock-pretreated cells and lipid treated cells (after SMase C pre-treatment). For all experiments, the geometric mean fluorescence of mock-treated cells (e.g. minus VacA) was subtracted from the geometric mean fluorescence of cells incubated with VacA.

Transfection of cells

AZ-521 cells were plated to 70–80% confluency after overnight incubation. After washing with PBS pH 7.2, cells were pre-incubated for 1 h with Opti-MEM® I (reduced serum, antibiotic-free medium; 200 μL; Invitrogen/GIBCO; Eugene, OR) at 37 °C and under 5% CO_2. Approximately 25 min prior to addition to cells, the appropriate dilutions of plasmid DNA and concentrated Lipofectamine (Invitrogen) were prepared according to the manufacturers instructions, and allowed to incubate for 5 min at 25 °C prior to mixing. Equal volumes of plasmid DNA and 6× Lipofectamine, both in Opti-MEM® I, were gently mixed, and incubated at 25 °C. After 20 min, the plasmid DNA-Lipofectamine mixture (100 μL) was added to each well in a drop-wise fashion with gentle agitation, and the cells were immediately incubated at 37 °C and under 5% CO_2. For these studies, AZ-521 cells were transfected with either pcDNA3- Cdc-42 (T17N)-GFP (0.4 μg per well) or pcDNA3-GFP (0.4 μg per well). After 6 h, Opti-MEM® I was removed from the monolayers, and the cells were incubated in complete medium at 37 °C and used immediately for the indicated studies. Using this protocol, we typically detected 60–80% of the cells within the monolayer to be transfected, as determined by visible EGFP fluorescence.

Cdc42 dependence of VacA internalization

AZ-521 cells were transfected with pcDNA3-Cdc-42 (T17N)-GFP or pcDNA3-GFP (both from Addgene Inc., Cambridge, MA), pretreated with SMase C, and then supplemented with C2-SM or C18-SM, as described above. The monolayers were incubated with either Alexa Fluor 647-labeled VacA (50 nM) or Alexa Fluor 568-labeled Tf (60 nM) to allow internalization for 30 min, and examined by DIC-epifluorescence microscopy. In transfected or non-transfected cells, as differentiated by the presence or absence of GFP fluorescence, respectively, the relative number of intracellular VacA-containing intracellular vesicles was quantified by directly counting red puncta from at least 10 cells in several different fields, and the data presented were combined from three independent experiments. The relative internalization was determined by calculating M_T/M_{NT}, which is the ratio of the mean number of VacA-containing intracellular vesicles in pcDNA3-Cdc-42 (T17N)-GFP transfected cells (M_T) to the mean number of VacA-containing intracellular vesicles in non-transfected cells (M_{NT}).

VacA co-localization with cellular trafficking markers

In 8-well chamber slides, 2×10^4 AZ-521 cells were plated in each well. After 24 h, the cells were pre-incubated in the presence of SMase C (50 mU/mL) at 37 °C. After 1 h, the monolayers were washed with ice-cold MEM containing 10% FBS to remove SMase C, and then further chilled on ice. The SMase C-treated cells were then further incubated for 30 min on ice in the absence or presence of pre-chilled C18-SM (25 μM) or C2-SM (25 μM) in complete medium. The cells were further incubated with prechilled Alexa Fluor 488-labeled VacA (50 nM) in the absence or presence of Alexa Fluor 568-labeled Tf (60 nM) or Alexa

Fluor 568-labeled ASSP (50 nM) on ice. In some experiments, cells were further incubated instead, as indicated, with Alexa Fluor 647-labeled VacA. After 1 h, the monolayers were washed one time with prechilled, complete medium plus unlabeled VacA (50 nM), and then further incubated at 37 °C with the addition of pre-warmed complete medium containing unlabeled VacA (50 nM). In other experiments, the cells were also incubated in the presence of Texas Red-labeled Dextran (1 μg/μL). At the indicated times, the cells were washed 3 times with ice-cold PBS pH 7.2, and then fixed with pre-chilled paraformaldehyde (4%) on ice. For each marker, co-localization was determined after incubation of the cells at 37 °C for 10, 30, 60, and 120 min. For studies requiring immunostaining, the fixed monolayers were first blocked using PBS pH 7.2 containing 2% BSA and then permeabilized by incubating with 0.1% Triton-X in PBS pH 7.2 for 10 min on ice, followed by incubation with rabbit polyclonal anti Rab-7, anti Rab-11, (1:500), or anti-Lamp-1 (1:200) antibodies (Santa Cruz Biotechnology, Inc. Santa Cruz, CA.), washed, and then further incubated with anti-mouse Alexa Fluor-488 (1:1000; Invitrogen).

Images were collected using wide-field fluorescence microscopy, as described above. Co-localization analysis was conducted by using the co-localization module of the DeltaVision SoftWoRx 3.5.1 software suite. Results were expressed as the colocalization index, which was derived from calculating the Pearson's coefficient of correlation values, which in these studies was a measure of co-localization between VacA and the indicated cellular marker in each z plane of the cell. For each cell, images from an average of 20–25 z planes at a thickness of 0.2 μM were collected. In these studies, a colocalization index value of 1.0 indicates 100% co-localization of VacA with the indicated cellular marker, whereas a co-localization index of 0.0 indicates the absence of co-localization of VacA with the indicated cellular marker. The colocalization index was calculated from the analysis of approximately ten cells from three independent experiments.

Preparation and analysis of DRMs

DRM preparation and analysis was performed as previously described (Lingwood and Simons, 2007; Patel *et al.*, 2002). DRMs were fractionated using OptiPrep® (Sigma) density centrifugation. AZ-521 cells (5×10^6 cells/mL in suspension) were incubated in the absence or presence of SMase C (50 mU/mL) at 37 °C. After 1 h, the cells were chilled to 0 °C and washed with ice-cold complete cellular medium to remove SMase C. The cells were then incubated on ice with C2-SM, C12-SM, or C18-SM (25 μM). After 30 min, the cells were further incubated on ice with pre-chilled VacA (100 nM). After 1 h, the cells were washed once with ice-cold complete cellular medium and collected by centrifugation at 300 × *g* at 4 °C for 5 min. The cell pellet was resuspended in ice-cold TNE buffer (25 mM Tris-HCl, 150 mM NaCl, 5 mM EDTA, pH 7.0) containing Protease Inhibitor Cocktail Set III (Calbiochem; La Jolla, CA). The suspended cells were lysed by fifteen passages through a 25-gauge needle. Membranes were solubilized by adding ice-cold Triton X-100 (1% final concentration in TNE) and incubating further at 4 °C on a rotary shaker. After 30 min, the lysates were adjusted to 40% Optiprep (600 μl) and loaded into the bottom of SW 40 Beckman tubes, overlaid with 1.2 mL of 30% Optiprep medium (TNE buffer), which was subsequently topped with 200 μl of TNE buffer. The gradients were centrifuged at 50,000 rpm and at 4 °C. After 2 h, raft and non-raft fractions (1.0 mL) were collected from the top to the bottom of the Optiprep gradient. The fractions were analyzed by SDS PAGE, and VacA were detected by Western blot analysis using VacA rabbit antiserum (Rockland Immunochemicals) and anti-rabbit IgG-alkaline phosphatase conjugate (Sigma). Flotillin was used as control for raft fractionation for OptiPrep gradients and detected by Western blot analysis using anti-flotillin-1 monoclonal antibody (BD Transduction Laboratories; San Jose, CA) and anti-mouse IgG-alkaline phosphatase conjugate (Sigma). The cross-reacting material was visualized after treating the blots with Lumi-phos (Pierce; Rockford, IL).

Statistics

Unless otherwise indicated, all data are representative of those obtained from at least three independent trials, each performed in triplicate. All statistical analyses were performed using Microsoft Excel (Version 11.0). Error bars represent standard deviations. All *P* values were calculated with the Student's *t* test using paired, two-tailed distribution. * indicates statistical significance ($P < 0.05$).

Supplementary Material

Refer to Web version on PubMed Central for supplementary material.

Acknowledgments

We thank Dr. F Gisou Van Der Goot (Ecole Polytechnique Federale de Lausanne) for the plasmid expressing SMase D, and Dr. E. Kiyokawa (Osaka U., Jp) for the plasmid expressing Venus-lysenin. We thank Dr. Tamilselvam Batcha and Mr. Prashant Jain for critical reading of the manuscript. This work was supported from a grant from the National Institutes of Health R01 AI045928 (to S.R.B.).

References

Barenholz, Y., editor. Sphingomyelin-lecithin balance in membranes: composition, structure, and function relationships. CRC Press; Boca Raton, FL: 1984.

Blanke SR. Portals and pathways: Principles of bacterial toxin entry into cells. Microbe. 2006; 1:26–32.

Cheng ZJ, Singh RD, Sharma DK, Holicky EL, Hanada K, Marks DL, Pagano RE. Distinct mechanisms of clathrin-independent endocytosis have unique sphingolipid requirements. Mol Biol Cell. 2006; 17:3197–3210. [PubMed: 16672382]

Chung JH, Lester RL, Dickson RC. Sphingolipid requirement for generation of a functional v1 component of the vacuolar ATPase. J Biol Chem. 2003; 278:28872–28881. [PubMed: 12746460]

Cover TL, Blanke SR. *Helicobacter pylori* VacA, a paradigm for toxin multifunctionality. Nature Reviews Microbiology. 2005; 3:320–332.

Cover TL, Blaser MJ. *Helicobacter pylori* in health and disease. Gastroenterology. 2009; 136:1863–1873. [PubMed: 19457415]

Cover TL, Hanson PI, Heuser JE. Acid-induced dissociation of VacA, the *Helicobacter pylori* vacuolating cytotoxin, reveals its pattern of assembly. J. Cell. Biol. 1997; 138:759–769. [PubMed: 9265644]

Cover TL, Puryear W, Perez-Perez GI, Blaser MJ. Effect of urease on HeLa cell vacuolation induced by *Helicobacter pylori* cytotoxin. Infect. Immun. 1991; 59:1264–1270. [PubMed: 2004808]

Cover TL, Vaughn SG, Cao P, Blaser MJ. Potentiation of *Helicobacter pylori* vacuolating toxin activity by nicotine and other weak bases. J Infect Dis. 1992; 166:1073–1078. [PubMed: 1402018]

de Bernard M, Papini E, de Filippis V, Gottardi E, Telford J, Manetti R, et al. Low pH activates the vacuolating toxin of *Helicobacter pylori*, which becomes acid and pepsin resistant. J. Biol. Chem. 1995; 270:23937–23940. [PubMed: 7592587]

Fivaz M, Vilbois F, Thurnheer S, Pasquali C, Abrami L, Bickel PE, et al. Differential sorting and fate of endocytosed GPI-anchored proteins. Embo J. 2002; 21:3989–4000. [PubMed: 12145200]

Fujikawa A, Shirasaka D, Yamamoto S, Ota H, Yahiro K, Fukada M, et al. Mice deficient in protein tyrosine phosphatase receptor type Z are resistant to gastric ulcer induction by VacA of *Helicobacter pylori*. Nat Genet. 2003; 33:375–381. [PubMed: 12598897]

Futter CE, Pearse A, Hewlett LJ, Hopkins CR. Multivesicular endosomes containing internalized EGF-EGF receptor complexes mature and then fuse directly with lysosomes. J Cell Biol. 1996; 132:1011–1023. [PubMed: 8601581]

Garner JA, Cover TL. Binding and internalization of the *Helicobacter pylori* vacuolating cytotoxin by epithelial cells. Infect Immun. 1996; 64:4197–4203. [PubMed: 8926088]

Gauthier NC, Ricci V, Landraud L, Boquet P. *Helicobacter pylori* VacA toxin: a tool to study novel early endosomes. Trends Microbiol. 2006; 14:292–294. [PubMed: 16730444]

Gauthier NC, Monzo P, Kaddai V, Doye A, Ricci V, Boquet P. *Helicobacter pylori* VacA cytotoxin: a probe for a clathrin-independent and Cdc42-dependent pinocytic pathway routed to late endosomes. Mol Biol Cell. 2005; 16:4852–4866. [PubMed: 16055501]

Gauthier NC, Ricci V, Gounon P, Doye A, Tauc M, Poujeol P, Boquet P. Glycosylphosphatidylinositol-anchored proteins and actin cytoskeleton modulate chloride transport by channels formed by the *Helicobacter pylori* vacuolating cytotoxin VacA in HeLa cells. J Biol Chem. 2004; 279:9481–9489. [PubMed: 14676190]

Gauthier NC, Monzo P, Gonzalez T, Doye A, Oldani A, Gounon P, et al. Early endosomes associated with dynamic F-actin structures are required for late trafficking of *Helicobacter pylori* VacA toxin. J Cell Biol. 2007; 177:343–354. [PubMed: 17438076]

Geisse NA, Cover TL, Henderson RM, Edwardson JM. Targeting of *Helicobacter pylori* vacuolating toxin to lipid raft membrane domains analysed by atomic force microscopy. Biochem J. 2004a; 381:911–917. [PubMed: 15128269]

Geisse NA, Cover TL, Henderson RM, Edwardson JM. Targeting of *Helicobacter pylori* vacuolating toxin to lipid raft membrane domains analysed by atomic force microscopy. Biochem J. 2004b; Pt

Genisset C, Puhar A, Calore F, de Bernard M, Dell'Antone P, Montecucco C. The concerted action of the *Helicobacter pylori* cytotoxin VacA and of the v-ATPase proton pump induces swelling of isolated endosomes. Cell Microbiol. 2007; 9:1481–1490. [PubMed: 17253977]

Gupta VR, Patel HK, Kostolansky SS, Ballivian RA, Eichberg J, Blanke SR. Sphingomyelin functions as a novel receptor for *Helicobacter pylori* VacA. PLoS Pathog. 2008; 4:e1000073. [PubMed: 18497859]

He X, Chen F, McGovern MM, Schuchman EH. A fluorescence-based, high-throughput sphingomyelin assay for the analysis of Niemann-Pick disease and other disorders of sphingomyelin metabolism. Anal Biochem. 2002; 306:115–123. [PubMed: 12069422]

Hed J, Hallden G, Johansson SG, Larsson P. The use of fluorescence quenching in flow cytofluorometry to measure the attachment and ingestion phases in phagocytosis in peripheral blood without prior cell separation. J Immunol Methods. 1987; 101:119–125. [PubMed: 3112235]

Kiyokawa E, Baba T, Otsuka N, Makino A, Ohno S, Kobayashi T. Spatial and functional heterogeneity of sphingolipid-rich membrane domains. J Biol Chem. 2005; 280:24072–24084. [PubMed: 15840575]

Koivusalo M, Alvesalo J, Virtanen JA, Somerharju P. Partitioning of pyrene-labeled phospho- and sphingolipids between ordered and disordered bilayer domains. Biophys J. 2004; 86:923–935. [PubMed: 14747328]

Koivusalo M, Jansen M, Somerharju P, Ikonen E. Endocytic trafficking of sphingomyelin depends on its acyl chain length. Mol Biol Cell. 2007; 18:5113–5123. [PubMed: 17942604]

Kuo CH, Wang WC. Binding and internalization of *Helicobacter pylori* VacA via cellular lipid rafts in epithelial cells. Biochem Biophys Res Commun. 2003; 303:640–644. [PubMed: 12659867]

Lafourcade C, Sobo K, Kieffer-Jaquinod S, Garin J, van der Goot FG. Regulation of the V-ATPase along the endocytic pathway occurs through reversible subunit association and membrane localization. PLoS One. 2008; 3:e2758. [PubMed: 18648502]

Lakadamyali M, Rust MJ, Zhuang X. Ligands for clathrin-mediated endocytosis are differentially sorted into distinct populations of early endosomes. Cell. 2006; 124:997–1009. [PubMed: 16530046]

Li Y, Wandinger-Ness A, Goldenring JR, Cover TL. Clustering and redistribution of late endocytic compartments in response to *Helicobacter pylori* vacuolating toxin. Mol Biol Cell. 2004

Lingwood D, Simons K. Detergent resistance as a tool in membrane research. Nat Protoc. 2007; 2:2159–2165. [PubMed: 17853872]

McClain MS, Schraw W, Ricci V, Boquet P, Cover TL. Acid activation of *Helicobacter pylori* vacuolating cytotoxin (VacA) results in toxin internalization by eukaryotic cells. Mol Microbiol. 2000; 37:433–442. [PubMed: 10931337]

Merrill AH Jr. De novo sphingolipid biosynthesis: a necessary, but dangerous, pathway. J Biol Chem. 2002; 277:25843–25846. [PubMed: 12011104]

Milhas D, Clarke CJ, Hannun YA. Sphingomyelin metabolism at the plasma membrane: Implications for bioactive sphingolipids. FEBS Lett. 2009

Molinari M, Galli C, Norais N, Telford JL, Rappuoli R, Luzio JP, Montecucco C. Vacuoles induced by *Helicobacter pylori* toxin contain both late endosomal and lysosomal markers. J. Biol. Chem. 1997; 272:25339–25344. [PubMed: 9312153]

Nakayama M, Hisatsune J, Yamasaki E, Nishi Y, Wada A, Kurazono H, et al. Clustering of *Helicobacter pylori* VacA in lipid rafts, mediated by its receptor, receptor-like protein tyrosine phosphatase beta, is required for intoxication in AZ-521 Cells. Infect Immun. 2006; 74:6571–6580. [PubMed: 17030583]

Nakayama M, Kimura M, Wada A, Yahiro K, Ogushi K, Niidome T, et al. *Helicobacter pylori* VacA activates the p38/activating transcription factor 2-mediated signal pathway in AZ-521 cells. J Biol Chem. 2004; 279:7024–7028. [PubMed: 14630932]

Niemela PS, Hyvonen MT, Vattulainen I. Influence of chain length and unsaturation on sphingomyelin bilayers. Biophys J. 2006; 90:851–863. [PubMed: 16284257]

Papini E, Zoratti M, Cover TL. In search of the *Helicobacter pylori* VacA mechanism of action. Toxicon. 2001; 39:1757–1767. [PubMed: 11595638]

Papini E, de Bernard M, Milia E, Bugnoli M, Zerial M, Rappuoli R, Montecucco C. Cellular vacuoles induced by *Helicobacter pylori* originate from late endosomal compartments. Proc. Natl. Acad. Sci. U S A. 1994; 91:9720–9724. [PubMed: 7937879]

Papini E, Satin B, Bucci C, de Bernard M, Telford JL, Manetti R, et al. The small GTP binding protein rab7 is essential for cellular vacuolation induced by *Helicobacter pylori* cytotoxin. EMBO J. 1997; 16:15–24. [PubMed: 9009263]

Patel HK, Willhite DC, Patel RM, Ye D, Williams CL, Torres EM, et al. Plasma membrane cholesterol modulates cellular vacuolation induced by the *Helicobacter pylori* vacuolating cytotoxin. Infect Immun. 2002; 70:4112–4123. [PubMed: 12117919]

Ricci V, Sommi P, Fiocca R, Romano M, Solcia E, Ventura U. *Helicobacter pylori* vacuolating toxin accumulates within the endosomal- vacuolar compartment of cultured gastric cells and potentiates the vacuolating activity of ammonia. J Pathol. 1997; 183:453–459. [PubMed: 9496263]

Ricci V, Galmiche A, Doye A, Necchi V, Solcia E, Boquet P. High cell sensitivity to *Helicobacter pylori* VacA toxin depends on a GPI-anchored protein and is not blocked by inhibition of the clathrin- mediated pathway of endocytosis. Mol. Biol. Cell. 2000; 11:3897–3909. [PubMed: 11071915]

Sabharanjak S, Sharma P, Parton RG, Mayor S. GPI-anchored proteins are delivered to recycling endosomes via a distinct cdc42-regulated, clathrin-independent pinocytic pathway. Dev Cell. 2002; 2:411–423. [PubMed: 11970892]

Sahlin S, Hed J, Rundquist I. Differentiation between attached and ingested immune complexes by a fluorescence quenching cytofluorometric assay. J Immunol Methods. 1983; 60:115–124. [PubMed: 6406600]

Salama NR, Otto G, Tompkins L, Falkow S. Vacuolating cytotoxin of *Helicobacter pylori* plays a role during colonization in a mouse model of infection. Infect Immun. 2001; 69:730–736. [PubMed: 11159961]

Schraw W, Li Y, McClain MS, van der Goot FG, Cover TL. Association of *Helicobacter pylori* vacuolating toxin (VacA) with lipid rafts. J Biol Chem. 2002; 277:34642–34650. [PubMed: 12121984]

Suerbaum S, Josenhans C. *Helicobacter pylori* evolution and phenotypic diversification in a changing host. Nat Rev Microbiol. 2007; 5:441–452. [PubMed: 17505524]

Telford JL, Ghiara P, Dell'Orco M, Comanducci M, Burroni D, Bugnoli M, et al. Gene structure of the *Helicobacter pylori* cytotoxin and evidence of its key role in gastric disease. J Exp Med. 1994; 179:1653–1658. [PubMed: 8163943]

Valsecchi M, Mauri L, Casellato R, Prioni S, Loberto N, Prinetti A, et al. Ceramide and sphingomyelin species of fibroblasts and neurons in culture. J Lipid Res. 2007; 48:417–424. [PubMed: 17093290]

van Meer G, Lisman Q. Sphingolipid transport: rafts and translocators. J Biol Chem. 2002; 277:25855–25858. [PubMed: 12011105]

Yahiro K, Niidome T, Hatakeyama T, Aoyagi H, Kurazono H, Padilla PI, et al. *Helicobacter pylori* vacuolating cytotoxin binds to the 140-kDa protein in human gastric cancer cell lines, AZ-521 and AGS. Biochem. Biophys. Res. Commun. 1997; 238:629–632. [PubMed: 9299564]

Yahiro K, Niidome T, Kimura M, Hatakeyama T, Aoyagi H, Kurazono H, et al. Activation of *Helicobacter pylori* VacA toxin by alkaline or acid conditions increases its binding to a 250-kDa receptor protein-tyrosine phosphatase beta. J Biol Chem. 1999; 274:36693–36699. In Process Citation. [PubMed: 10593974]

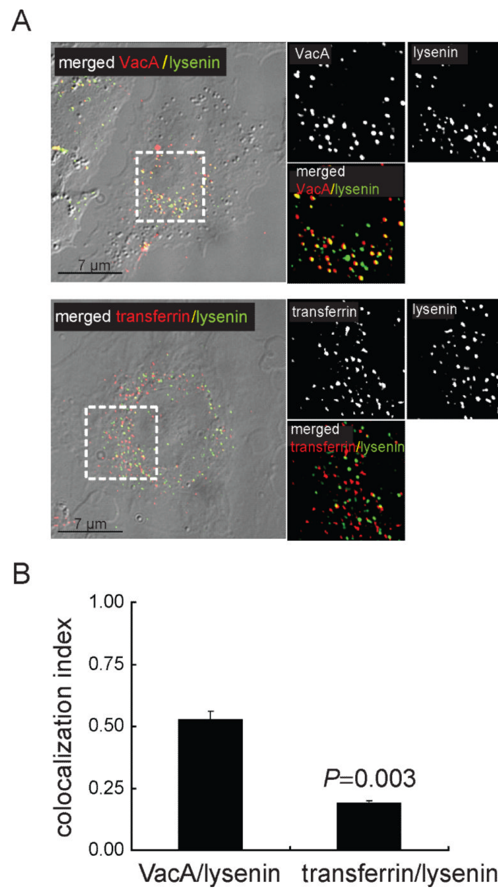

Fig. 1.

SM is associated with VacA-containing intracellular vesicles.

Co-localization of Alexa Fluor 647 labeled-VacA (50 nM) or Alexa Fluor 568 labeled-transferrin (60 nM) in AZ-521 cells with Venus-lysenin (1 μM) after 30 min was determined as described under Experimental Procedures.

A. Images were collected using DIC-fluorescence microscopy. The areas within the dashed white box were enlarged to illustrate VacA only (red puncta), transferrin only (red puncta), Venus-lysenin only (green puncta), colocalized VacA-Venus-lysenin (yellow puncta), or colocalized transferrin-Venus-lysenin (yellow puncta).

B. Co-localization analysis was carried out for the studies described in (A) as described under Experimental Procedures. The results shown were derived from data combined from three independent experiments. Statistical significance was calculated for differences in the colocalization index between those cells incubated with VacA and Venus-lysenin (VacA-Venus-lysenin) and those cells incubated with transferrin and Venus-lysenin (transferrin-Venus-lysenin).

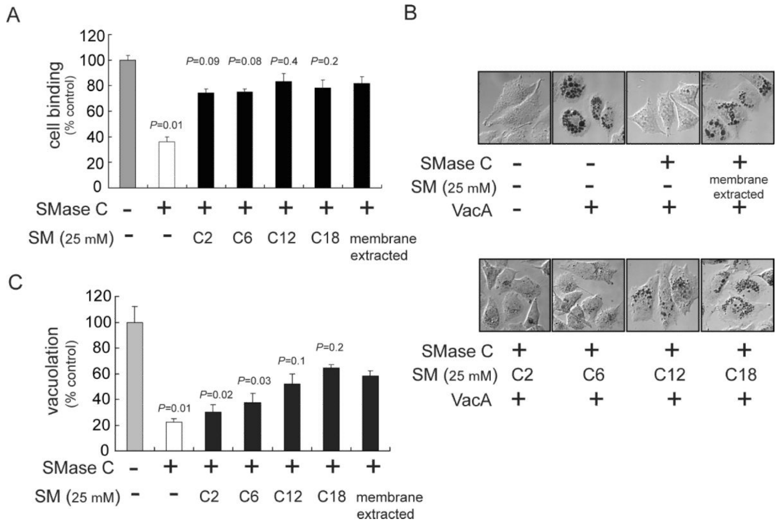

Fig. 2.

Effects of SM acyl chain length on cell binding and sensitivity to VacA.

AZ-521 cells were incubated with SMase C (50 mU/mL) for 1 h at 37 °C, and then chilled on ice to 0 °C. The cells were washed with ice-cold complete cell medium to remove SMase C. The cells were then incubated for 30 min on ice in the absence or presence of pre-chilled C2-SM, C6-SM, C12-SM, C18-SM, or membrane extracted SM (all at 25 μM). The cells were further incubated with prechilled Alexa Fluor 488-labeled VacA (50 nM) (A) or unlabeled VacA (50 nM) (B,C). After 1 h, the cells were analyzed for VacA binding (A) or further incubated at 37 °C and under 5% CO_2 (B,C).

A. The level of VacA binding was determined using flow cytometry. Cell binding was calculated by determining the geometric mean fluorescence intensities of each sample. The results shown were derived from data combined from three independent experiments in which binding was normalized to control cells that had been mock-pretreated with complete cell medium prior to VacA binding. Statistical significance was calculated for differences in VacA binding between those cells pretreated sequentially with SMase C alone or SMase C and acyl chain variants of SM, and, those cells pretreated with SMase C and then “membrane extracted” SM.

B. After 8 h, the cells were stained with neutral red and visualized using DIC microscopy.

C. Cellular vacuolation was quantified using the neutral red assay. The results shown were derived by normalizing neutral red uptake to that measured in control cells that had been mock-pretreated with complete cell medium prior to VacA binding. Statistical significance was calculated for differences in vacuolation between those cells pretreated sequentially with SMase C alone or SMase C and acyl chain variants of SM, and, those cells pretreated with SMase C and then “membrane extracted” SM.

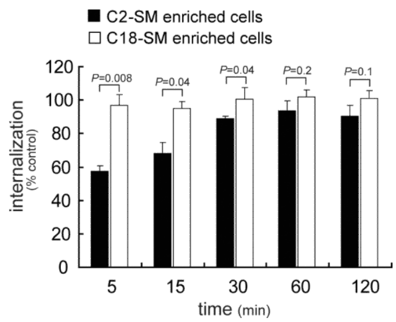

Fig. 3.

Effects of SM acyl chain length on the rate of VacA internalization.

AZ-521 cells that had been enriched with either C2-SM or C18-SM were evaluated for internalized Alexa Fluor 488-labeled VacA (50 nM) using flow cytometry, as described under “Experimental Procedures.” The results shown were derived by normalizing the amount of internalized VacA to that measured in control cells that had been mock-pretreated with complete cell medium prior to incubation with VacA (data not shown). Statistical significance was calculated for differences in internalized VacA at each time point between those cells enriched in C2-SM (black bars) and those cells enriched in C18-SM (empty bars).

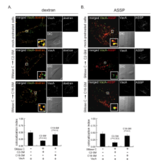

Fig. 4.
Effects of SM acyl chain length on VacA localization with fluid phase- and GPI-anchored proteins-enriched intracellular vesicles.
DIC-fluorescence microscopy images were collected and co-localization of Alexa Fluor 488-labeled VacA with Texas Red-labeled dextran (A) or Alexa Fluor 568-labeled ASSP (B) after internalization for 10 min into AZ-521 cells supplemented with either C2-SM or C18-SM was determined, as described under "Experimental Procedures." Within the larger merged images of VacA and dextran (A) or ASSP (B), the areas within the dashed white box were enlarged as solid white boxes located in the lower, right hand corners of the merged images, to illustrate VacA (green puncta), dextran or ASSP (red puncta), or VacA co-localized with either dextran or ASSP (yellow-colored puncta). The white puncta in the smaller black and white images illustrate, as labeled, VacA (A, B), dextran (A), or ASSP (B). The smaller, lower panels are the DIC images provided to illustrate the overall shape of the cell(s), and include the black scale bars. The co-localization index was determined for VacA with dextran (A) or VacA with ASSP (B). The results shown were derived from data combined from three independent experiments. Statistical significance was calculated for differences in the colocalization index between those cells enriched in either C2-SM or C18-SM and those cells that had been mock-pretreated only.

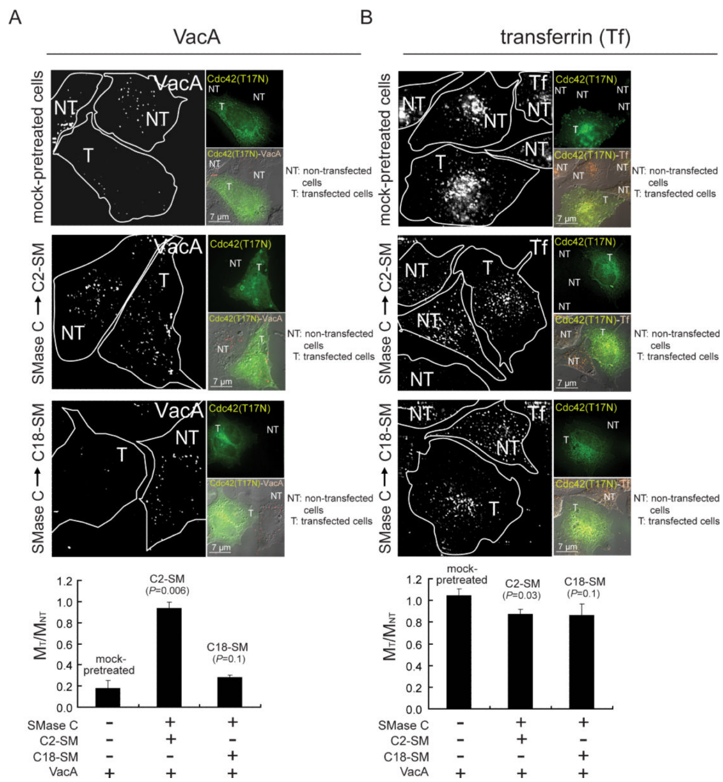

Fig. 5.

Effects of SM acyl chain length on Cdc42-dependent internalization of VacA.

Alexa Fluor 647-labeled VacA (50 nM) (A) or Alexa Fluor 568-labeled Tf (60 nM) (B) was visualized using DIC fluorescence microscopy after internalization for 30 min into AZ-521 cells that had been transfected with pcDNA3-Cdc-42 (T17N)-GFP and then supplemented with either C2-SM or C18-SM, as described under "Experimental Procedures." The images were rendered to include in each field at least one transfected (T) and non-transfected (NT) cell as indicated, respectively, by the presence or absence of cellular green fluorescence. In the larger images, the boundaries of each cell are outlined in white. The top smaller panels indicate transfected cells, as indicated by the green fluorescence due to pcDNA3-Cdc-42 (T17N)-GFP. The gray scale bars are included in the bottom smaller panels, which show DIC images along with pcDNA3-Cdc-42 (T17N)-GFP (green; A, B) and VacA puncta (red; A) or transferrin (orange, Tf; B). The number of visible fluorescent white puncta were counted within individual cells, and used to calculate M_T/M_{NT}, which is the ratio of fluorescent puncta between transfected and untransfected cells. M_T/M_{NT} values were derived from data combined from three independent experiments. Statistical significance was calculated for differences in M_T/M_{NT} between those cells enriched in either C2-SM or C18-SM, and, those cells that had not been pretreated.

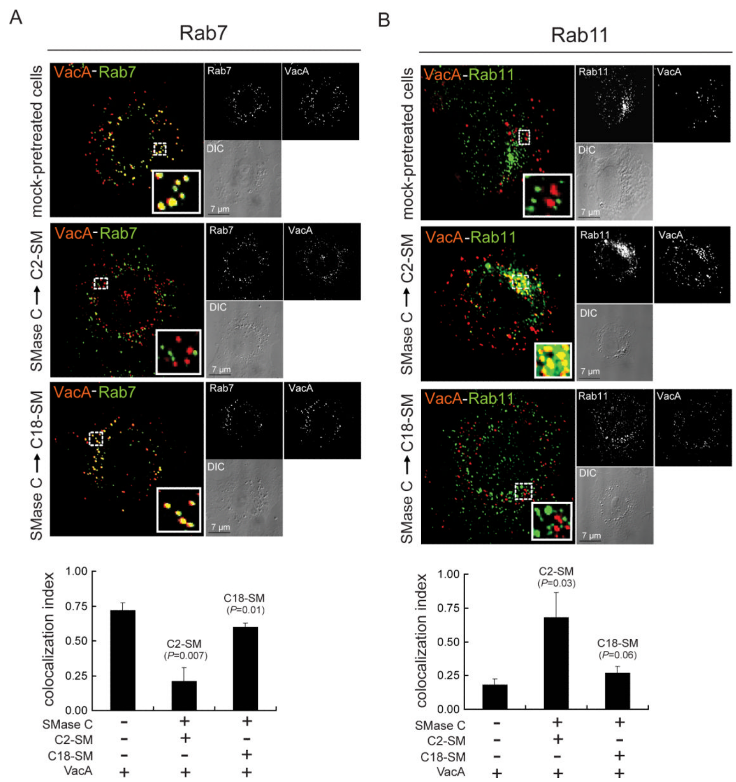

Fig. 6.

Localization of VacA to intracellular vesicles enriched in Rab7 or Rab11 is sensitive to variation in SM acyl chain length.

Intracellular Alexa Fluor 647 labeled VacA (50 nM) was visualized for co-localization with Rab7 (A) or Rab11 (B) using DIC fluorescence microscopy after internalization for 120 min (A) or 30 min (B) into AZ-521 cells that had been supplemented with either C2-SM or C18-SM, as described under "Experimental Procedures." Within the larger merged images of VacA and Rab7 (A) or Rab11 (B), the areas within the dashed white box were enlarged as solid white boxes located in the lower, right hand corners of the merged images, to illustrate VacA (red puncta), Rab7 or Rab11 (green puncta), or VacA co-localized with either Rab7 or Rab11 (yellow-colored puncta). The white puncta in the smaller, upper black and white images illustrate, as labeled, VacA (A, B), Rab7 (A), or Rab11 (B). The smaller, bottom panels are the DIC images provided to illustrate the overall shape of the cell(s), and include the black scale bars. The colocalization index was determined for VacA with Rab7 (A) or VacA with Rab11 (B) in cells enriched in C2-SM, cells enriched in C18-SM, or cells that had not been pretreated prior to incubation with VacA. The colocalization index values were derived from data that had been combined from three independent experiments. Statistical significance was calculated for differences in the colocalization between VacA and Rab7 (VacA-Rab7) (A), and, VacA and Rab11 (VacA-Rab11) (B).

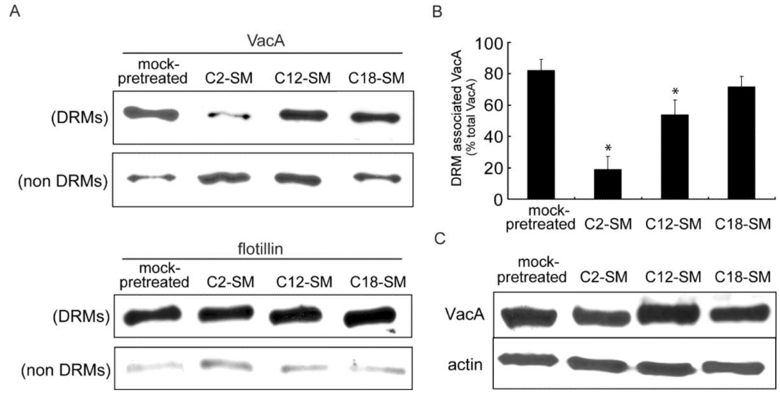

Fig. 7.

Effects of SM acyl chain length on VacA distribution in rafts.

AZ-521 cells were incubated with SMase C (50 mU/mL) for 1 h at 37 °C, and then chillled on ice to 0 °C. The cells were washed with ice-cold-medium to remove SMase C. The cells were then incubated in the presence of C2-SM, C12-SM, or C18-SM (25 μM) for 30 min on ice. The cells were further incubated with prechilled VacA (100 nM) for 1 h on ice, washed once with ice-cold medium, and lysed and analyzed for raft and non-raft proteins as described under Experimental Procedures.

(A) Western blot analysis of VacA and flotillin in DRM and non-DRM fractions of lysed cells.

(B) Fraction of VacA in DRM and non-DRM fractions of lysed cells as determined by densitometry analysis of Western blots. These results are rendered from the combined data obtained from three independent experiments. Statistical significance was calculated for differences between the cross-reacting material present in the DRMs and non-DRMs.

(C) Western blots analysis of VacA and actin cross-reacting material from total lysates of cells enriched in C2-SM, C12-SM, C18-SM, or mock-pretreated cells.